

Computation with chaos: A paradigm for cortical activity

(attentiveness/categorization/motion detection)

A. BABLOYANTZ AND C. LOURENÇO

Service de Chimie-Physique, Université Libre de Bruxelles, CP 231 Campus Plaine, Boulevard du Triomphe, B-1050 Bruxelles, Belgium

Communicated by I. Prigogine, May 20, 1994

ABSTRACT A device comprising two interconnected networks of oscillators exhibiting spatiotemporal chaos is considered. An external cue stabilizes input specific unstable periodic orbits of the first network, thus creating an “attentive” state. Only in this state is the device able to perform pattern discrimination and motion detection. We discuss the relevance of the procedure to the information processing of the brain.

Electrical activity of cerebral cortex can be measured non-invasively from the scalp. The electroencephalograms (EEGs) thus obtained are local averaged activity of millions of cells. According to the behavioral states of the brain, the EEG shows well-defined ethology. Some pathologies such as, for example, the “petit-mal” epilepsy or Creutzfeld-Jakob coma generate very characteristic waves. Thus, before the advent of more sophisticated medical imagery techniques the EEG was a diagnostic tool for assessing neurological diseases. It still is a common tool for assessing sleep disorders.

In the past decade the techniques of nonlinear time series analysis were applied by Babloyantz and her colleagues to the human EEG (1–4). They could show that in several behavioral states as well as in petit-mal epilepsy and Creutzfeld-Jakob coma the EEG may be described by deterministic chaotic dynamics. Several groups have confirmed the existence of chaotic dynamics in the human cortex (see refs. 5 and 6 and references therein).

Drawing on these findings a model of cerebral cortex was recently constructed (7). In this model, the various behavioral states of the cortex are seen as spatiotemporal chaotic cortical activity of increasing coherence generated by the nature of the input from the thalamus. The space average of network activity over an area of the cortex provides EEG-like signals, which are akin to behavioral states of human brain activity. Such models led to the concept that the dynamics of cerebral cortex is of spatiotemporal chaotic nature. Thus, it seems that information processing in the brain is performed at a global network level. The information processing capacity of neuronal networks was demonstrated recently by measuring the active neuronal population in the *Aplysia* abdominal ganglion network during spontaneous and evoked behaviors using multineuronal optical measurements (8). It was found that a distributed organization involving a large number of neurons of the network may generate the two behaviors. These functional behaviors stem from altered activities of a large ensemble of neurons and thus they are a network property. This assumption raises the following question: If brain dynamics is of a chaotic nature then how does such a system process information?

The importance of providing an answer to this question is 2-fold. First, it may give a clue for the understanding of brain processes. Second, the relevant concepts could be integrated into artificial neural networks in order to produce a more

efficient computational device by mimicking more closely brain dynamics and its awesome capacity for storage and rapid processing of a great amount of complex information.

Indeed, the classical neural networks generally rely on fixed-point attractor dynamics, thus limiting the capacity of small or moderate-sized networks. On the other hand, chaotic dynamics, even with few degrees of freedom, can in principle provide an infinite means of coding, as it is a “reservoir” of an infinite number of unstable periodic orbits (9–11). In our approach, the periodic orbits are used as coding devices.

The aim of this paper is to propose a neural network model based on chaotic dynamics, which not only encompasses the parallel computation seen in brain dynamics but also introduces layered chaotic structures that exhibit somewhat more brain-like architecture and features such brain attributes as a state of attentiveness. Indeed, cerebral cortex is a multilayer structure with specific interconnections between different layers (12). Each layer is a network of densely connected neurons. Moreover, different layers are thought to have functional specificities in the processing of information, and it is widely assumed that information is embedded in the links or synapses joining the neurons. On the other hand, in all sensory processing the first task is to become receptive to incoming information. Once such an “attentive” state is reached, the information to be treated could flow through the specific pathways. For instance, in a busy airport it is perfectly possible to become oblivious to the environmental noise. A conversation extracted from the background noise will convey information only if one pays attention deliberately. This is also the case for the visual system. It is possible to look intensively at an object without seeing it. Seeing requires a deliberate will to become attentive. Once this attentive state is reached, the brain is ready to process the incoming information. Usually the attentive state is reached very rapidly and has a finite time span.

The model we propose is an interconnected two-layered device. Each layer is a chaotic network of oscillatory units. A small external or internal input brings the device into an attentive state. We show that once the device is in an attentive state, it can perform such tasks as pattern categorization, motion detection, and discrimination between clockwise and counterclockwise rotation. The dynamics of the device makes use of unstable periodic orbits contained in a chaotic attractor, which are stabilized by small fluctuations with the help of an algorithm proposed by Ott, Grebogi, and Yorke (13, 14). The number of such orbits is infinite; thus, even small chaotic networks may in principle process an infinite amount of information.

We begin by introducing the model and proceed to discussing pattern discrimination and motion detection. In a final section, we discuss the relevance of the model as a paradigm of brain function.

The publication costs of this article were defrayed in part by page charge payment. This article must therefore be hereby marked “advertisement” in accordance with 18 U.S.C. §1734 solely to indicate this fact.

Abbreviation: EEG, electroencephalogram.

MODEL

Chaotic Categorizer. Let us consider a device, hereafter called a chaotic categorizer, made of two interconnected layers as shown in Fig. 1 (15). Each layer comprises $N \times N$ oscillating elements. The elements of the two layers are connected in a one-to-one correspondence with links that are active and represent a given pattern only if an external stimulus activates the first layer. The details of this procedure will become apparent in the sequel.

The pacemaker P sends micropulses only to layer I as shown in Fig. 1. In the absence of external stimuli, the activities of the two layers are independent and both show spatiotemporal chaotic behavior.

The device is described by the following differential equations:

$$\begin{aligned} \frac{dZ_{jk}}{dt} &= Z_{jk} - (1 + i\beta)|Z_{jk}|^2Z_{jk} + (1 + i\alpha)D \sum_{l,m} C_{jklm}Z_{lm} + P_{jk}(t) \\ \frac{dW_{jk}}{dt} &= W_{jk} - (1 + i\beta)|W_{jk}|^2W_{jk} + (1 + i\alpha)D \sum_{l,m} C_{jklm}W_{lm} \\ &\quad + \gamma I_{jk}(Z_{jk} - W_{jk}) \quad (j, k, l, m = 1, \dots, N). \end{aligned} \quad [1]$$

The variables Z_{jk} are the complex amplitudes describing the oscillators in layer I , whereas W_{jk} refers to the corresponding variables in layer II . The first two terms in each equation are related to the complex Ginzburg-Landau description of amplitude equations for each oscillator. The diffusive connectivity C_{jklm} relating the oscillators is defined as

$$\sum_{l,m} C_{jklm}Z_{lm} = Z_{j(k+1)} + Z_{j(k-1)} + Z_{(j+1)k} + Z_{(j-1)k} - 4Z_{jk}.$$

The parameters α, β, D , and γ are real-valued. α and D reflect the coupling strength between units. The term $P_{jk}(t)$ represents the influence of the pacemaker P on each oscillator of layer I . The boundary conditions are of the zero-flux type.

The information to be processed is sent to the device via a binary matrix I_{jk} . If $I_{jk} = 0$ then the connection between elements jk of the two layers is nonexistent. However, if $I_{jk} = 1$ then the two layers are connected via elements jk , and γ describes the strength of the binding. Moreover, in this model if $P_{jk}(t) = 0$ then $\gamma = 0$. Thus, it is only when the pacemaker P is active, and therefore a periodic orbit has been stabilized in layer I , that there is entrainment of the second layer by the first layer. The entrainment can be total if all $I_{jk} = 1$, and it is partial if only some of the I_{jk} are nonzero. Moreover, the dynamics of the second layer is critically dependent on the parameter γ . If $\gamma = 0$ then the two layers have independent dynamics, whereas large values of γ with a large number of

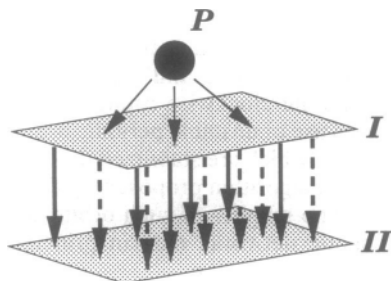


FIG. 1. Chaotic categorizer. The pacemaker P sends micropulses to layer I , thus stabilizing one of the unstable periodic orbits. The oscillators of layers I and II are connected with a one-to-one correspondence. The distribution of active links (solid arrows) and inactive ones (dashed arrows) is determined by a pattern to be processed. A response is measured from output layer II .

“on” links representing incoming information can synchronize the activities of the two layers.

If $P_{jk}(t) = 0$, $\gamma = 0$, $N = 9$, $\alpha = -10$, $\beta = 2$, and $D = 1.3$, then both layers follow spatiotemporal chaotic activity. The dynamics of each network separately could be viewed as evolving on a chaotic attractor embedded in a $2(N \times N)$ dimensional space. It is well known that such a strange attractor comprises an infinite number of unstable periodic orbits (9–11). Recently, with the help of a technique proposed by Ott, Grebogi, and Yorke (13), one could stabilize four different orbits out of the global attractor of the network by applying micropulses to the system with the help of the pacemaker P (14). Fig. 2 displays three orbits that exhibit spatiotemporal structure. The nature of the stabilized orbit is a function of the pacemaker P . More details can be found in ref. 14.

The orbit C_0 corresponds to the bulk oscillation of the network, where all the oscillators are in-phase. The period of this oscillation is $T = \pi$. Although the orbits C_1 , C_2 , and C_3 are periodic at the level of the $2N^2$ dimensional dynamics, when viewed at the network level they exhibit spatiotemporal structures. Phase differences are seen between individual oscillators of the network. The orbit C_1 with $T = 13.66$ shows a rotating wave activity of the amplitude of individual units around the central unit of the network. The amplitude of the latter is zero; that is, we are in the presence of a “phase defect.” In this case, the rotation is clockwise. The orbits C_2 and C_3 show stationary waves of different symmetries. Orbit C_2 is antisymmetric and shows a polar structure. The activity is high on one side and low on the opposite side. The situation reverses with constant period $T = 15.4$. In orbit C_3 , spatiotemporal phenomena show a different structure. The activity is high in units along one of the diagonals and near the corners of the network, whereas the oscillators on the other diagonal show lower activity close to the corners. Again, as in C_2 , the situation changes regularly with constant frequency. The period of C_3 is $T = 2.25$. In principle, an infinite number of other periodic orbits could be stabilized in this system. We have not considered them in this paper.

Let us go back to our device as shown in Fig. 1 and describe how it can process information. The total input into the system is divided into two parts. The pacemaker P , which emits the appropriate micropulses, and the input, which must be processed. Thus, the information is captured on the first layer and on the links relating the latter to the second layer.

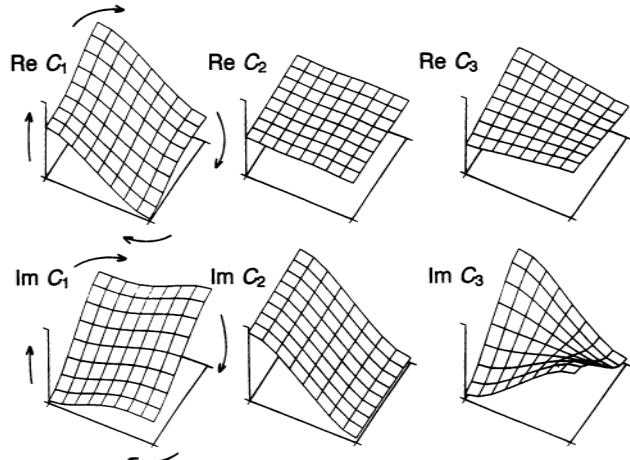


FIG. 2. Snapshots of network activity W corresponding to the unstable periodic orbits C_1 , C_2 , and C_3 with periods $T = 13.66$, 15.4 , and 2.25 , respectively. Vertical axes span the interval $[-1.2, 1.2]$. Parameter values are $N = 9$, $\alpha = -10$, $\beta = 2$, and $D = 1.3$. For orbit C_1 , arrows show the direction of rotation of the wave of activity (from ref. 14).

The response of the second layer defines the output of the system. The pacemaker P , according to the nature of the information to be processed, stabilizes the first layer into one of the orbits described in Fig. 2. In analogy with the human brain, where the first act in any cognitive process is to become attentive to an external input, we call these orbits the "attentive states" of the device. Now the device is ready for processing the input. The latter is imprinted in the links I_{jk} , which are nonzero only if they represent a part of the input. The attentive state, which represents well-defined spatiotemporal structure, entrains the output layer according to the number and location of "on" links in the device. Thus, in the second layer each input pattern generates its own specific spatiotemporal structure.

The dynamics of the output layer can remain chaotic or be of a quasi-periodic or periodic nature. To discriminate between various inputs, we need to quantify the spatiotemporal activity of the response layer. Unfortunately, so far there are no satisfactory methods for quantification of spatiotemporal chaotic activity. However, as we are interested in the differential change in the network coherence of layer II as a result of the input, the evaluation of the global activity of that layer will be sufficient. Throughout this paper we use the average value of the squared amplitude of the forced layer $\langle |W|^2 \rangle(t)$ as the output function. The brackets $\langle \rangle$ denote a space average over the entire network.

We have also computed other quantities such as the mean value of the real part of W over the network. The time evolution of the cross-correlation function between the two layers was also computed. It is defined as

$$C(t) = \text{Re} \frac{\sum_{j,k} Z_{jk}(t) W_{jk}(t)}{(\sum_{j,k} |Z_{jk}(t)|^2)^{1/2} (\sum_{j,k} |W_{jk}(t)|^2)^{1/2}}$$

In our simulations, the function $\langle |W|^2 \rangle(t)$ seemed in general more appropriate for pattern and motion discrimination than the other monitored functions.

The chaotic categorizer of Fig. 1 can be used as a pattern recognition device as well as a motion detector. The ability of the device to perform a given task is a function of the attentive state that is generated by the device under the action of the input to be processed. With our categorizer the orbits C_2 and C_3 are suitable for pattern recognition and also for detection of linear motion, whereas C_1 is an orbit that leads to detection of clockwise and counterclockwise motion.

RESULTS

Pattern Discrimination. All three attentive states brought about by orbits C_1 , C_2 , and C_3 are suitable in some degree for pattern discrimination. However, because of symmetries inherent in orbits C_2 and C_3 , these are more suitable than C_1 for pattern processing.

We start with the device in the attentive state C_2 . In this state, the stabilized orbit in the first layer shows a polarity that oscillates in time. At a given time one may see a high activity at the right hand side of the network, while the activity is at its lowest level at the left hand side. The situation reverses periodically. In this attentive state, the device is presented with a bar that activates the nine middle links between the two layers and is parallel to the direction of polarity of the orbit C_2 . When these links are "on" there follows an entrainment of layer II by layer I. The value of the space average $\langle |W|^2 \rangle$ is a measure of this entrainment and is shown in Fig. 3. One sees a constant value of 0.68. In another experiment, the bar is presented again to the middle links of the network but perpendicularly to the polarity of C_2 . The response of the system as seen in Fig. 3 is irregular, with high amplitude and a decreased mean value. If the bar is presented

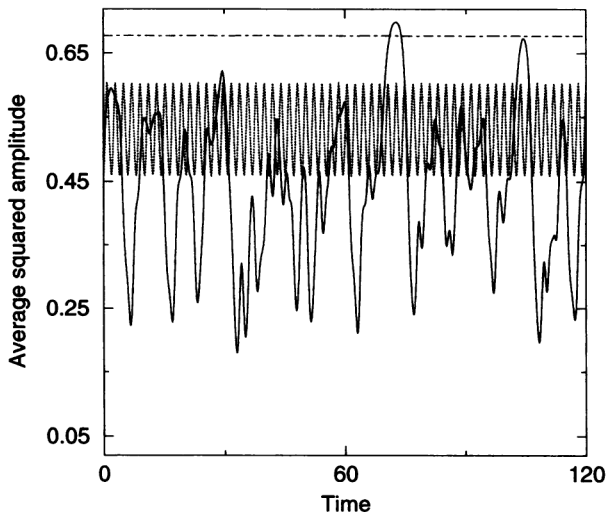


FIG. 3. Space average of the squared amplitude $\langle |W|^2 \rangle$ measured from layer II. Orbit C_2 is stabilized in layer I. Three patterns are presented to the device: a bar activating the nine middle links and parallel to the direction of polarity of C_2 (dot-dashed line), a bar activating nine links perpendicularly to the direction of polarity (solid line), and a bar activating nine links along one of the diagonals of the network (dotted line). $\gamma = 2.44$; all other parameters are as in Fig. 2.

along the diagonal, the response is periodic with a time averaged value of 0.53 (see also Fig. 3). Therefore, our simple device when in the attentive state C_2 can discriminate between different orientations on the plane.

If the same type of experiment is conducted in the attentive state C_3 , the device can discriminate only between a bar perpendicular to the side of the network and one presented along the diagonal. This property stems from the fact that orbit C_3 has a reflection symmetry with respect to the two diagonals and therefore the two axes perpendicular to the side of the network entrain layer II in the same manner. Because of the quasi-circular symmetry of orbit C_1 , the corresponding attentive state is not suitable for the type of pattern processing mentioned above.

Fig. 4 shows the output of layer II when two patterns, + and \times , are presented to the system when it is in the attentive

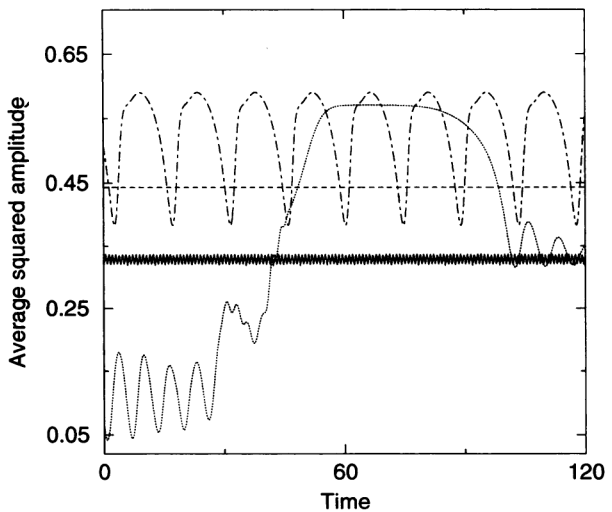


FIG. 4. Responses $\langle |W|^2 \rangle(t)$ of the output layer in the presence of the patterns + and \times . With orbit C_2 , the response is shown as a dot-dashed line for pattern + and as a dotted line for pattern \times . When orbit C_3 is used, the response corresponding to pattern + is shown as a dashed line, whereas the solid line is obtained with pattern \times . Parameter values are as in Fig. 3.

state C_2 . We see that the two patterns are discriminated by the system. The same is true for the attentive state C_3 (see Fig. 4). However, we notice that the form and amplitude of responses for a given pattern are not identical for the two attentive states.

Let us consider another pair of patterns, N and Z. The first letter can be recovered by a 90° rotation of the second. From symmetry considerations and the result of experiments with single bars, we expect that the attentive state C_2 will discriminate between patterns N and Z, whereas the state C_3 will give the same answer for both patterns. Our simulations confirmed these conjectures.

Motion Detection. The device of Fig. 1 is able to discriminate between clockwise and counterclockwise rotation. To this end we assume that the attentive state of the system is achieved by the stabilization of the first layer into orbit C_1 , which shows a phase rotation of period $T = 13.66$ (see Fig. 2). As we have stated already, in this example the phase motion of the stabilized orbit is clockwise. Because of the phase rotation of the orbit, the attentive state C_1 is able to discriminate between clockwise and counterclockwise motion.

To see this, let us consider the motion of a small object that activates three links at a time. In this experiment, $\gamma = 30$. As the object moves, only the next neighboring link is activated and one of the previous "on" links is deactivated. Thus, the successive activation and deactivation of links represents a circular motion. In our example, the diameter of the circular trajectory spans over five network units and the rotation period of the object varies from $T = 6$ to $T = 25$.

In a first experiment, when in the attentive state C_1 , the device perceives the clockwise motion of the object, which is imprinted in the links. The response of layer II is shown in Fig. 5 when the period of rotation of the object is $T = 18.96$. The value of the space average of the squared amplitude $\langle |W|^2 \rangle = 0.65$ is almost constant in time. However, at very fine resolution small-amplitude oscillations are seen around this value (not apparent in Fig. 5). The same response is seen for all values of the rotation periods considered. Thus, in the attentive state C_1 , the device is not sensitive to the speed of clockwise motion of the object.

Presently we reverse the direction of rotation of the object and keep all other conditions as described above. The re-

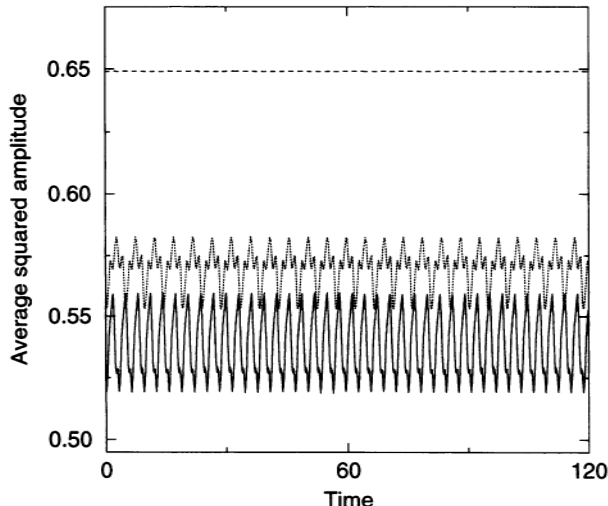


FIG. 5. $\langle |W|^2 \rangle(t)$ computed in the attentive state C_1 for a clockwise (dashed line) and a counterclockwise (dotted line) motion with period of rotation $T = 18.96$. If the object rotates in the counterclockwise direction with a period $T = 12.48$ (solid line), a higher amplitude response with a lower time average value is seen. $\gamma = 30$; other parameters are as in Fig. 2.

sponse of layer II to counterclockwise motion is very different and is sensitive to the rotation speed. For $T = 6$ the motion generates a chaotic response ($\langle |W|^2 \rangle$) around a time-averaged value of 0.5. As the speed decreases, the time behavior of the response becomes less and less chaotic and gradually a time periodic output function appears. Fig. 5 shows the responses associated with the counterclockwise motions of periods $T = 12.48$ and $T = 18.96$. The corresponding time-averaged values of $\langle |W|^2 \rangle$ are 0.54 and 0.57, respectively. For the range of T considered, the value of $\langle |W|^2 \rangle$ corresponding to counterclockwise motion is always smaller than that for clockwise motion. The time-averaged value and the shape of the response in the case of counterclockwise motion are sensitive to the speed of rotation. If we restrict the range of T to $12 < T < 25$, we observe that the time-averaged value of $\langle |W|^2 \rangle$ is an increasing function of T . Thus, in this range not only our device discriminates between clockwise and counterclockwise motion, but it also evaluates the speed of counterclockwise motion. For slow motions, $T > 26$, and very fast motions, $T < 0.5$, the response to clockwise and counterclockwise rotation is practically identical. A difference may be seen only in the fine structure of the $\langle |W|^2 \rangle$ output function. Thus, for these velocities the device is "blind" with respect to the direction of rotation. The responses in these ranges are similar to the response to clockwise rotation for $6 < T < 24$ (see Fig. 5). For values of $0.5 < T < 6$, the response of the system does not follow the smooth change that was described above. A static object could be considered as rotating with period $T \rightarrow \infty$ and thus it is perceived in the same manner as other objects rotating with long periods—that is, $T > 26$.

Motion detection is not limited to the orbit C_1 . The attentive states corresponding to orbits C_2 and C_3 are able to perceive a moving object and discriminate between perpendicular and diagonal motions.

Let us consider the attentive state C_3 and a moving object that activates only one link at a time. The motion starts from the middle of the boundary of the device and continues along a straight line perpendicular to that boundary. Each link is activated during 11 time units. The response of layer II is monitored in the usual way and is markedly different from the one when the object moves along the diagonal. However, opposite directions of motion along any one of these paths cannot be distinguished. With orbit C_3 the two perpendicular orientations cannot be distinguished, and the same happens regarding the two diagonal ones. The distinction between the two perpendicular orientations is possible only if the device is in the attentive state C_2 . The latter is also unable to discriminate between the two opposite directions along any one of the two diagonals as well as along each of the two perpendicular axes.

DISCUSSION

We have shown that a simple device, made of two interconnected layers of oscillators and featuring spatiotemporal chaotic dynamics, is capable of pattern selection and motion detection. This capability is intrinsic to the system and is unsupervised. As a result of algorithmic complexities inherent in the Ott–Grebogi–Yorke method, in this simple example only three orbits with spatiotemporal structure and the bulk oscillation were stabilized in the first layer. However, in principle there are an infinite number of unstable orbits in a chaotic attractor that could be stabilized. With the stabilization of higher-order orbits one would expect more intricate symmetries or more complex spatiotemporal phenomena, especially if larger networks are considered. Thus, one would think that such a chaotic device could process a great variety of information relative to static as well as moving objects.

Spatiotemporal chaos may arise also in artificial neural networks. Usually one tries to avoid such situations in

classical computational techniques, as chaos is perceived generally as a nuisance. Instead of avoiding chaos, we believe that more elaborate devices, based on principles underlined in this paper, could make chaotic dynamics a desirable tool for unsupervised computations. Chaotic attractors are loci of an infinite number of unstable periodic orbits. Therefore, even small networks may exhibit high capacity.

Another important aspect of our model is that it is a paradigm for understanding some aspects of cerebral cortical activity. The system described in this paper embodies several key features of cortical architecture, which consists of interconnected layers of neurons, each layer with its own specific input-output pathways. On the other hand, measurements from EEGs as well as model systems and the nature of cortical tissue suggest that the activity at the cortical layers could be of a spatiotemporal chaotic nature (1–7). Moreover, all information processing becomes possible if one is in a state of attentiveness. This state can be reached by external or internal cues.

Building on the properties of our device, let us speculate on the nature of the state of attentiveness in cerebral cortex. We propose that the first effect of any sensory cue is to stabilize one or several unstable periodic orbits in one of the cortical layers that we call the layer of attentiveness. Any sensory cue may be thought of as a sum of different elements, each representing a particular feature of incoming information and thus stabilizing a specific orbit. This fact is plausible in view of the layered structure of the cortex. For example, a given sensory cue can stabilize all three orbits of Fig. 2, each in one sheet of neurons of the attentiveness layer. This in turn implies that in the presence of a sensory cue the attentiveness layer switches from a chaotic or turbulent state to a more coherent state, which is a superposition of well-defined oscillatory modes. Overall, one may see a much more synchronized activity in one of the layers of the cortex during the attentive state. Only when such a coherent state is reached may other cortical areas become active and process the relevant information.

We believe the theory we propose could be tested experimentally in the following manner. During *in vivo* animal experiments, a vertical battery of electrodes could be implemented chronically in a well-defined area of the sensory cortex—for example, the visual cortex. The multielectrodes span several layers and sublayers of the cortex. One records from all electrodes simultaneously in the absence of sensory cues. The field potentials could then be analyzed by several techniques of nonlinear time series analysis (1–4). The values of dynamical parameters such as entropies and Lyapunov exponents and dimensions characterize the dynamics of the signal. A second measurement is performed by presenting a sensory cue to the animal, and the same type of quantitative analysis is repeated. If our conjecture is correct, then the comparison of data from each layer will show an increase in coherence—that is, a more synchronized dynamics—in one of the layers. Such an experiment will show the existence of an attentiveness layer and can determine its location in the cortex.

Another consequence of our conjecture is that the incoming information is processed by other layers of the cortex in

the form of specific spatiotemporal activities such as limit cycles, coherent propagation phenomena, and spatiotemporal chaos with various degrees of coherence. This is in sharp contrast with the manner in which computation is performed in classical artificial neural networks. Experimental data pointing in this direction have been reported in the literature (16–18).

Recently, we could show that stabilization of unstable periodic orbits could be achieved in model systems describing more adequately the cortical tissue (19). This model takes account of propagation delays in neuronal transmission between excitatory and inhibitory neurons, which are not oscillating units. The ideas expressed above must presently be tested with these more brain-like networks.

We thank J. A. Sepulchre for interesting discussions. C.L. acknowledges the support of the Portuguese Government (Junta Nacional de Investigações Científicas e Tecnológicas—Programa CIENCIA, BD/1765/91-IA). This work was also supported in part by the Belgian Government (IMPULSE Project RFO AI 10, Calcul de Puissance Project IT/SC/25) and the European Economic Community (ESPRIT, Basic Research, 3234).

1. Babloyantz, A., Salazar, J. & Nicolis, C. (1985) *Phys. Lett. A* **111**, 152–156.
2. Babloyantz, A. & Destexhe, A. (1986) *Proc. Natl. Acad. Sci. USA* **83**, 3513–3517.
3. Babloyantz, A. (1991) *Electroencephalogr. Clin. Neurophysiol.* **78**, 402–405.
4. Gallez, D. & Babloyantz, A. (1991) *Biol. Cybernet.* **64**, 381–391.
5. Roschke, J. & Basar, E. (1989) in *Brain Dynamics*, Springer Series in Brain Dynamics, eds. Basar, E. & Bullock, T. H. (Springer, Berlin), Vol. 2, pp. 131–148.
6. Rapp, P. E., Bashore, T. R., Martiner, J. M., Albano, A. M., Zimmerman, I. D. & Mees, A. I. (1989) *Brain Topogr.* **2**, 99–118.
7. Destexhe, A. & Babloyantz, A. (1991) *Neural Comput.* **3**, 145–154.
8. Wu, J., Cohen, L. & Falk, C. (1994) *Science* **263**, 820–823.
9. Ruelle, D. (1985) *Thermodynamic Formalism* (Addison-Wesley, Reading, MA).
10. Auerbach, D., Cvitanović, P., Eckmann, J.-P., Gunaratne, G. & Procaccia, I. (1987) *Phys. Rev. Lett.* **58**, 2387–2389.
11. Pawelzik, K. & Schuster, H. (1991) *Phys. Rev. A* **43**, 1808–1812.
12. Churchland, P. S. & Sejnowski, T. J. (1989) *The Computational Brain* (MIT Press, Cambridge, MA).
13. Ott, E., Grebogi, C. & Yorke, J. (1990) *Phys. Rev. Lett.* **64**, 1196–1199.
14. Sepulchre, J. A. & Babloyantz, A. (1993) *Phys. Rev. E* **48**, 945–950.
15. Babloyantz, A. & Sepulchre, J. A. (1993) in *Proceedings of the International Conference on Artificial Neural Networks, Amsterdam, The Netherlands, 13–16 September 1993*, eds. Gielen, S. & Kappen, B. (Springer, London), pp. 670–675.
16. Rougeul-Buser, A., Bouyer, J., Montaron, M. & Buser, P. (1983) in *Exp. Brain Res. Suppl.* **7**, 69–87.
17. Eckhorn, R., Bauer, R., Brosch, M., Jordan, W., Kruse, W., Munk, M. & Reitboeck, H. (1988) *Invest. Ophthalmol. Vis. Sci.* **29**, 331–343.
18. Gray, C., König, P., Engel, A. & Singer, W. (1989) *Nature (London)* **338**, 334–337.
19. Lourenço, C. & Babloyantz, A. (1994) *Neural Comput.* **6**, 1140–1153.